

The Influence of Geometry on Linear Damping*

by M. E. McIntyre and J. Woodhouse

Department of Applied Mathematics and Theoretical Physics, University of Cambridge

Summary

Internal damping of vibration modes of bodies such as plates and shells generally depends on mode shape, boundary conditions and geometry. This dependence is explored systematically using linear continuum mechanics, exploiting the differences between different complex moduli which are frequently ignored, particularly in isotropic materials. Detailed results are given for isotropic plates, of constant and slightly varying thickness, under various boundary conditions. One prediction of the theory is tested experimentally, and good agreement is obtained. Effects of the kind described appear to be of great importance in the construction of musical instruments of the violin family, and they deserve attention in any situation where Q 's of vibration modes are required to be accurately known.

Einfluß der Geometrie auf die lineare Dämpfung

Zusammenfassung

Die innere Dämpfung von Schwingungsmoden in Platten und Schalen hängt allgemein von der Modenform, den Randbedingungen und der Geometrie ab. Diese Abhängigkeit wird unter Verwendung der linearen Kontinuumsmechanik systematisch untersucht, wobei die oft übersehenen Unterschiede, insbesondere für isotrope Materialien, zwischen verschiedenen komplexen Modulen ausgewertet werden. Für isotrope Platten konstanter sowie leicht variierender Dicke und für verschiedene Randbedingungen werden detaillierte Ergebnisse angegeben. Bei der experimentellen Überprüfung einer aus der Theorie abgeleiteten Beziehung ergab sich gute Übereinstimmung. Effekte der beschriebenen Art scheinen von großer Bedeutung für die Konstruktion von Musikinstrumenten aus der Violinenfamilie zu sein und sie verdienen darüber hinaus immer dann Beachtung, wenn die Q 's von Schwingungsmoden genau bekannt sein müssen.

Influence de la configuration géométrique sur l'amortissement linéaire

Sommaire

L'amortissement interne des modes de vibration de corps tels que les plaques et les coques dépend généralement de la forme du mode, des conditions aux limites et de la configuration géométrique. On explore systématiquement cette dépendance par le moyen de la théorie linéaire de la mécanique des milieux continus, en recourant aux différences entre les divers modules complexes. Ces différences sont en général négligées, surtout s'agissant de matériaux isotropes. On donne des résultats détaillés pour les plaques isotropes d'épaisseur constante ou légèrement variable, pour diverses conditions aux limites. L'une des prédictions de la théorie est comparée avec les résultats expérimentaux, et l'accord est bon. Les effets du type décrit semblent devoir être importants pour la construction d'instruments de musique de la famille du violon, et ils méritent qu'on s'y arrête dans toutes les circonstances où il est nécessaire de connaître avec précision les facteurs de qualité de modes vibratoires.

1. Introduction

In most engineering situations where the internal damping of vibration is important, the main concern is to maximise this damping, for example to limit the amplitude of parasitic vibrations or to reduce colouration in loudspeakers. The work described here is fundamental to some of these problems, but it was originally motivated by experimental findings in a context where elaborate pains are taken to achieve, inter alia, precisely the opposite effect, namely to minimise the internal

damping of certain vibration modes of a structure. The findings are those of Hutchins [1], who has examined some of the traditional procedures of the violin-maker. It appears that when the back and front plates of an instrument are being hollowed out, the maker arrives at a best thickness distribution for each by frequently tapping it and listening,

* Paper presented in April 1976 to the 91st meeting of the Acoustical Society of America and abstracted in *J. Acoust. Soc. Amer.* 59 [1976], Supplement 1, pp. S34 and S36.

aiming for a "clear, full ring": this subjective judgement must involve among other things a heuristic observation of internal damping. A remarkable feature is the sensitivity of the procedure: sometimes a difference can be heard as a result of removing just 0.1 mm of wood from a few square centimetres of a plate of some 3 mm thickness. An interesting conclusion of Hutchins is that subjectively good results can be achieved by confining attention to certain of the gravest modes of the free plates, despite the fact that their frequencies occupy only a small part of the audible range. Most surprising of all is that optimising an aspect of the behaviour of the individual free plates should have a decisive and desirable effect on the finished violin, since the plates will behave quite differently under the different boundary conditions in the assembled instrument.

In this paper we discuss the basic phenomenon from a fundamental continuum-mechanics viewpoint, using linear theory. We also investigate whether and when related effects might occur in more familiar engineering situations. It might be thought that the highly anisotropic material and complicated geometry of violin plates are essential to the behaviour described; however, continuum-mechanical considerations immediately show that even homogeneous isotropic materials can, in principle, be expected to display variations of Q with specimen geometry, boundary conditions and individual mode shape. In section 3 below we give measurements on rectangular, constant-thickness plates of an approximately isotropic material, displaying Q -variations (of some 20%) in close accordance with the pattern predicted by the theory.

Our starting point is to write down the general form of the dependence of Q on the geometrical factors of the problem. One can then enquire how sensitive this dependence is, in various cases of interest. That is, how much can the Q 's vary with geometry and mode shape, for a given material? This in turn requires us to answer a related question: how many material parameters must be measured in order to be able to predict Q 's for all modes and geometries of this material? The general theory tells us that at least two damping measurements are needed (at a given frequency) for isotropic materials, while for orthotropic materials nine are needed. (Four, however, suffice for orthotropic thin plates containing two of the symmetry axes of the material.) This contrasts with the two measurements usually made on wood (e.g. Barducci and Pasqualini [2]). We conclude that as yet insufficient information is available about the damping properties of

wood to predict with confidence the psycho-acoustically important properties of stringed instruments.

2. General theory, and the application to flat, isotropic plates

Whenever linear theory is valid for small-amplitude motions of a general continuum, we may restrict attention to time-harmonic oscillations in which stress and strain both have the time dependence $e^{i\omega t}$. This allows the (linear) relationship between the stress and strain tensors to be expressed in the same form as in linear elasticity theory, provided that the coefficients involved are made complex and allowed to be functions of frequency ω ¹. The number N of independent complex coefficients (or more familiarly "complex moduli") is restricted by the symmetries of the material in the usual way. Thus we have the "correspondence principle" of linear viscoelasticity theory (using the term to include all linear hysteretic effects) as enunciated by, for example, Bland [3]: "if a linear elastic problem in which all time dependence is of a form $e^{i\omega t}$ can be solved by a method which does not involve separating real and imaginary parts, then the solution of the corresponding problem for a given viscoelastic material is obtained from the elastic solution simply by replacing the elastic constants occurring in it by suitable complex functions of frequency which characterise that particular viscoelastic material". These complex moduli may readily be visualised in terms of frequency-dependent phase-lags in the response of a specimen to an applied sinusoidal stress of suitable form. It is emphasised that the foregoing involves no assumptions whatever beyond that of linearity.

We are concerned with eigenvalue problems for the normal modes of vibration of bodies. Suppose we have solved an elastic problem, obtaining an eigenfunction $w(\mathbf{x}; K_1^0, \dots, K_N^0)$ with corresponding eigenvalue $\omega_0 = \Lambda(K_1^0, \dots, K_N^0)$ where K_1^0, \dots, K_N^0 (with N as above) are a complete set of elastic constants for the material considered, and \mathbf{x} is position. (Of course, not all problems will involve the entire set of K 's.) Then the corresponding linear problem for any viscoelastic material will have an eigenfunction $w[\mathbf{x}; K_1(\omega), \dots, K_N(\omega)]$ where the eigenvalue ω is the solution of

$$\omega = \Lambda[K_1(\omega), \dots, K_N(\omega)] \quad (2.1)$$

and where

$$K_1(\omega), \dots, K_N(\omega) \quad (2.2)$$

¹ Indeed they must be ω -dependent, to satisfy the principle of causality (e.g. Scanlan [4]).

are complex moduli corresponding to the elastic constants K_1^0, \dots, K_N^0 . The viscoelastic solution will thus differ from the elastic one in two ways: first, the eigenfunction will have a continuous distribution of phase over the specimen, seen explicitly by writing

$$w(\mathbf{x}) = |w(\mathbf{x})| e^{i\varphi(\mathbf{x})} \quad (2.3)$$

where $\varphi(\mathbf{x})$ is a real function, and second, the eigenvalue will now be complex, so that the vibration is damped. (The requirement of damping, rather than exponential growth, for all eigenmodes gives us constraints on admissible functions $K_n(\omega)$ for real materials: see for example relations (2.24) below.)

We cannot hope to solve eq. (2.1) exactly. Even for elastic problems which can be solved analytically the functional dependence $A(K_1^0, \dots, K_N^0)$ is usually unobtainable in explicit form from the eigenvalue equation, and in any case eq. (2.1) is an implicit equation for ω which would be intractable for realistic functions $K_n(\omega)$. Thus we resort to the approximation of small damping,

$$\text{Re}(\omega) \gg \text{Im}(\omega) \quad (2.4)$$

requiring

$$|K_n^0| \gg |K_n'|, \quad n = 1, \dots, N \quad (2.5)$$

where

$$K_n'(\omega) = \text{Im}[K_n(\omega)]. \quad (2.6)$$

In other words, nearly-elastic behaviour is assumed. This should be reasonably accurate for the Q -values around 80 encountered in violin plates, as well as for many engineering situations. A larger range of Q 's could be dealt with by iterating eq. (2.1), if necessary.

To extract useful information from this approximation we use Rayleigh's variational principle, as this directly gives, in a sense which proves convenient, the functional dependence $A(K_1^0, \dots, K_N^0)$ of ω_0 upon K_n^0 . Recall that if an elastic problem has potential energy $V(w)$ and kinetic energy $\omega^2 T(w)$, then when w is an eigenfunction, we have

$$A^2 = V/T \quad (2.7)$$

for the corresponding eigenvalue, and the quotient on the right is stationary to small perturbations in w (Rayleigh [5], § 88).

To help fix ideas we now work in terms of a specific example, namely the isotropic flat plate, which will turn out to be the simplest system to exhibit the interesting behaviour we seek. (We will subsequently apply the same method to other systems: see section 6 and 7, and also Appendix 2.)

From Rayleigh [5], § 214, we know that a plate of density ρ with slowly-varying thickness $h(\mathbf{x})$ has, according to classical plate theory, the potential energy

$$V = \frac{1}{24} \int h^3 \{K_1^0 (\nabla^2 w)^2 - K_2^0 \mathcal{G} w\} dA, \quad (2.8)$$

where

$$K_1^0 = E^0 / \{1 - (\nu^0)^2\} \quad (2.9)$$

and

$$K_2^0 = 2E^0 / (1 + \nu^0)$$

in terms of Young's modulus E^0 and Poisson's ratio ν^0 , and $\mathcal{G} w$ is the Gaussian curvature of the displacement $w(\mathbf{x}) = w(x, y)$, and is defined by

$$\mathcal{G} w \equiv w_{xx} w_{yy} - w_{xy}^2. \quad (2.10)$$

It may be convenient to recall that, in terms of the principal radii of curvature R_1 and R_2 of the deformation,

$$\begin{aligned} \nabla^2 w &= (1/R_1) + (1/R_2), \\ \mathcal{G} w &= 1/R_1 R_2. \end{aligned} \quad (2.11)$$

The kinetic energy of our plate is

$$\omega_0^2 T = \frac{1}{2} \rho \omega_0^2 \int h w^2 dA. \quad (2.12)$$

Thus the Rayleigh quotient (2.7) reduces in this case to

$$\begin{aligned} \omega_0^2 &= A^2(K_1^0, K_2^0) = \\ &= \frac{\int h^3 \{K_1^0 (\nabla^2 w)^2 - K_2^0 \mathcal{G} w\} dA}{12 \rho \int h w^2 dA}, \end{aligned} \quad (2.13)$$

where $w(\mathbf{x}; K_1^0, K_2^0)$ is an eigenfunction. The right hand side is stationary with respect to small departures $\delta w(\mathbf{x})$ from the form of the eigenfunction. Now note that just such a small change, albeit complex, is induced in $w(\mathbf{x})$ if we change the material from an elastic one to a viscoelastic one satisfying eq. (2.5). Thus the value of the Rayleigh quotient becomes complex, but the contribution from the change in $w(\mathbf{x})$ is small compared to that from the change in K_1 and K_2 , so that taking imaginary parts and dividing by ω_0^2 we have

$$\begin{aligned} \frac{\text{Im}(\omega^2)}{\omega_0^2} &= \frac{K_1' \int h^3 (\nabla^2 w)^2 dA - K_2' \int h^3 \mathcal{G} w dA}{12 \rho \omega_0^2 \int h w^2 dA} + \\ &+ O\left(\frac{K_1'}{K_1^0}\right)^2 + O\left(\frac{K_2'}{K_2^0}\right)^2, \end{aligned} \quad (2.14)$$

where the integrals are evaluated using the elastic eigenfunction $w(\mathbf{x})$. We can conveniently write this in terms of dimensionless quantities by introducing the Q of the resonance, where

$$Q^{-1} = 2 \text{Im}(\omega) / \text{Re}(\omega) \approx \text{Im}(\omega^2) / \omega_0^2. \quad (2.15)$$

Then

$$Q^{-1} \approx (K_1' / K_1^0) I_1 + (K_2' / K_2^0) I_2, \quad (2.16)$$

where the dimensionless quantities

$$I_1 = \frac{K_1^0 \int h^3 (\nabla^2 w)^2 dA}{12 \rho \omega_0^2 \int h w^2 dA} \geq 0 \tag{2.17a}$$

and

$$I_2 = \frac{-K_2^0 \int h^3 \mathcal{G} w dA}{12 \rho \omega_0^2 \int h w^2 dA}. \tag{2.17b}$$

Note that, from eq. (2.13),

$$I_1 + I_2 = 1. \tag{2.18}$$

For isotropic materials with K_1'/K_1^0 not equal to K_2'/K_2^0 eq. (2.16) tells us what mixture of the two is appropriate to a given situation. The quantities I_1 and I_2 are invariants (i.e. do not depend on the coordinate system used) which are known in terms of the elastic solution only. They are properties of the plate geometry and boundary conditions, and the particular mode in question, containing all the relevant information about damping under the small-damping approximation (2.5). Any parameter of the problem which affects the ratio $I_1 : I_2$ can change the value of Q , so that we have established the possibility of behaviour similar to that in the violin plates, but in isotropic materials. To discuss such effects, we have only to investigate the behaviour of $I_1 : I_2$ in the elastic problem and then apply eq. (2.16).

We see immediately from eqs. (2.16) and (2.18) that the magnitude of the effect for a given material is determined by the difference between K_1'/K_1^0 and K_2'/K_2^0 . A convenient dimensionless measure of the difference is

$$\gamma \equiv \frac{K_1'/K_1^0 - K_2'/K_2^0}{K_1'/K_1^0}. \tag{2.19}$$

With this definition, eq. (2.16) can be rewritten with the help of eq. (2.18) as

$$Q^{-1} = Q^{-1}|_{I_2=0} \times (1 - \gamma I_2). \tag{2.20}$$

So γ is a dimensionless material property which gives a general idea of the possible fractional variation of Q among different modes, since for each mode I_2 is a number of order unity. (Moreover, $I_2 \leq 1$ by eqs. (2.17a) and (2.18), and has in fact been found to lie within the range $(-0.7, +0.98)$ for all plate modes whose eigenfunctions we have calculated so far.)

We can relate γ to the complex bulk and shear moduli k and μ as follows. Define

$$\alpha = \frac{k'/k^0}{\mu'/\mu^0}. \tag{2.21}$$

Then it is readily shown with the aid of the standard formulae connecting k , μ , E and ν that

$$\gamma \approx \frac{(1 + \nu^0)(1 - 2\nu^0)}{(1 + \nu^0)(1 - 2\nu^0) - 3(1 - \nu^0)(1 - \alpha)^{-1}}, \tag{2.22}$$

to within the small-damping approximation (2.5). Note that $\gamma = 0$ if $\alpha = 1$, i.e. if $k'/k^0 = \mu'/\mu^0$.

From first principles

$$-1 \leq \nu^0 \leq 0.5 \tag{2.23}$$

and

$$\mu'/\mu^0 > 0, \quad k'/k^0 > 0, \tag{2.24}$$

for a physically possible material (stable to all small deformations). From relations (2.24),

$$\alpha > 0. \tag{2.25}$$

It is now readily shown from relations (2.22) to (2.25) that

$$-0.5 \leq \gamma \leq 1. \tag{2.26}$$

The detailed behaviour of γ for $0 \leq \alpha \leq 2$ is shown in Fig. 1 for various values of ν^0 . (γ is insensitive to ν^0 near $\nu^0 = 0$ because eq. (2.22) implies that $d\gamma/d\nu^0 = 0$ at $\nu^0 = 0$, for all α .)

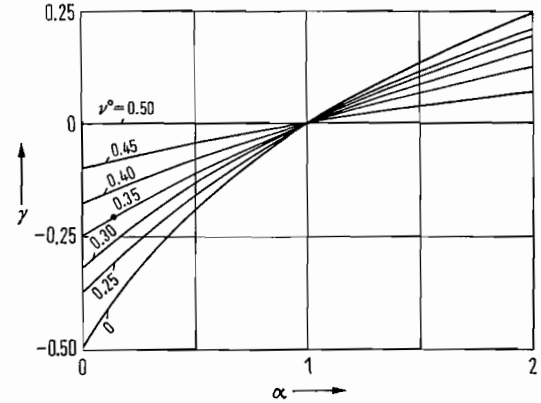


Fig. 1. The sensitivity γ of Q to mode shape for flat isotropic plates: $Q^{-1} = Q^{-1}|_{I_2=0} \times (1 - \gamma I_2)$, where I_2 is a number characterising the mode shape and usually lying between ± 1 . The curves are labelled with different values of Poisson's ratio ν^0 . The point at $\gamma = -0.21$, $\nu^0 = 0.35$ corresponds to the experiment on ABS described in section 3.

We would naturally like to know more precisely what values γ can take in real materials, in particular what sign it has. To achieve this we must use empirical information: for example Snowdon [6], p. 7, states that in "rubber-like" materials $\alpha \ll 1$, implying negative γ . When this is true, it appears from Fig. 1 that geometric effects on damping should be most marked in materials with low values of Poisson's ratio. However, "rubber-like" usually entails near-incompressibility (ν^0 close to 0.5), so it may be that for most materials $|\gamma|$ will be around 0.2 or less. This is probably what lies behind the usual engineer's approximation, which is simply to set $\gamma = 0$, and ignore these effects entirely (e.g. Lazan [7], § 2.5), since in many applications Q -variations of perhaps 20% are not

of great interest. This is not, however, the case with musical instruments.

We note for later reference the relation between γ and ν' , the imaginary part of Poisson's ratio:

$$\frac{\nu'}{1 - \nu^0} = \frac{K_1'}{K_1^0} \gamma. \quad (2.27)$$

3. Experimental test of the predictions

We now discuss a direct experimental test of eq. (2.16). The simplest method is to find a specimen geometry for which I_2 varies for the different modes of vibration, so that we can simply measure Q for each mode and plot Q^{-1} against calculated values of I_2 , expecting a linear relation from eq. (2.20). We shall find later that the simplest arrangement which produces mode-to-mode variation of I_2 is a rectangular, free-edged plate of constant thickness. (It would be easier to make measurements on bars or thin strips, but we shall see in section 6 that these do not serve the purpose.)

We first compute the elastic eigenfunctions of such a plate, and calculate I_2 for each one: the numerical method used and the checks made on its accuracy are discussed in Appendix 1. Results for the case of a square plate are summarised in

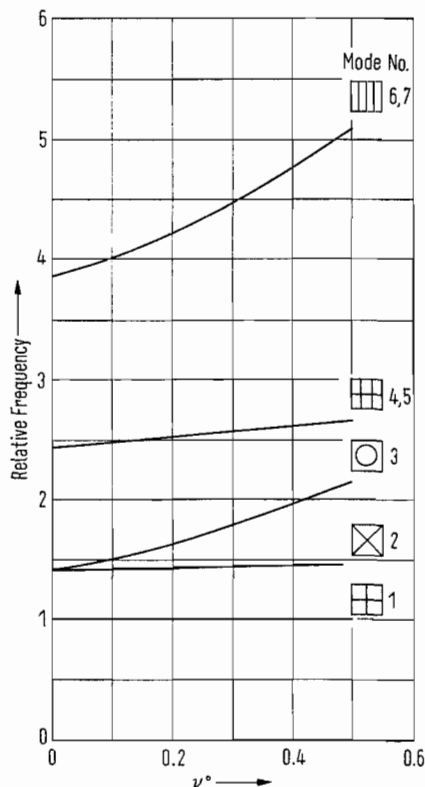


Fig. 2. Graph of the frequencies of normal modes of a square, free-edged, isotropic elastic plate, relative to that of the gravest mode, against Poisson's ratio ν^0 .

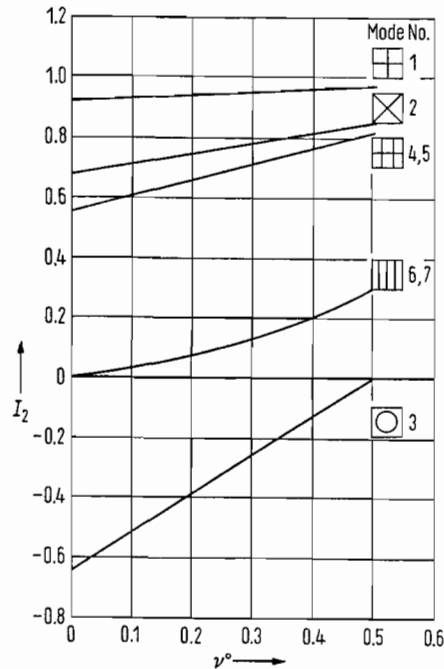


Fig. 3. Graph of I_2 against Poisson's ratio for normal modes of a square, free-edged, isotropic elastic plate.

Figs. 2 and 3. Fig. 2 is a graph of eigenfrequencies relative to that of the gravest mode, plotted against Poisson's ratio ν^0 : this is needed to calculate ν^0 from measured mode frequencies. Then the values of I_2 for each mode are taken from Fig. 3, where they are plotted against ν^0 . Other values of I_2 for a given ν^0 can be obtained from rectangular plates of different proportions: as the plate becomes longer and thinner, I_2 for all low modes tends to $2\nu^0/(1 + \nu^0)$ (see section 6).

We now describe some simple measurements of Q^{-1} for the corresponding modes of real plates using a digital data processing technique. The response of the plate to an impulse is registered by a Bruel and Kjaer 8307 miniature accelerometer and fed into an Alpha LSI-2 mini-computer via an analogue-to-digital converter. When suitable time has elapsed after the impulse for the plate to be vibrating freely, successive segments of the signal are fast-Fourier-transformed and plotted on a visual display unit. The program then locates peaks in the curves and fits exponential decays to the time-variation of the peak values, thence calculating Q for the mode in question, after checking that the decay is indeed exponential to sufficient accuracy. The plate is then scaled to bring the next mode to the same frequency, and the measurement repeated for this mode. The main error in the method comes from the finite sampling resolution of the analogue-to-digital converter, but this is a true

random error which can be greatly reduced by averaging the results of repeated measurements. Apart from this, timing accuracy is guaranteed by the computer's master crystal clock, which gives a great advantage over measurement techniques relying on the calibration of analogue oscillators (such as half-power bandwidth measurements).

The chief difficulty with the measurements lies in finding a method of suspending the plate so that it achieves a reasonable approximation to free boundary conditions. To achieve the potential measurement accuracy of about 2% for Q 's of the order of 80, great care has to be taken with this. The best method we have been able to use involved drilling small holes in the plate at intersections of node lines of two relevant modes and measuring Q 's for these modes with the plate suspended on light threads through these holes.

Other unwanted effects sufficiently large to be detectable in some situations were found to be radiation damping, and interference between modes of similar frequencies. In addition, most sheet materials are by no means homogeneous or isotropic in practice, so it was hardly surprising that the results for some specimens had a large scatter. Acrylics such as perspex are particularly bad in this respect.

Of the rather small range of test materials available to us, the behaviour predicted by eqs. (2.16) and (2.20) is most clearly exhibited by ABS plastic sheet (polymerized acrylonitrile butyl styrene). Fig. 4 is a graph of Q^{-1} against I_2 for a few modes of plates of this material, the plates of varying proportions being cut from the same piece, since different specimens vary. Measured Q 's ranged from 66 to 83, and with $\nu^0 \approx 0.35$ (from

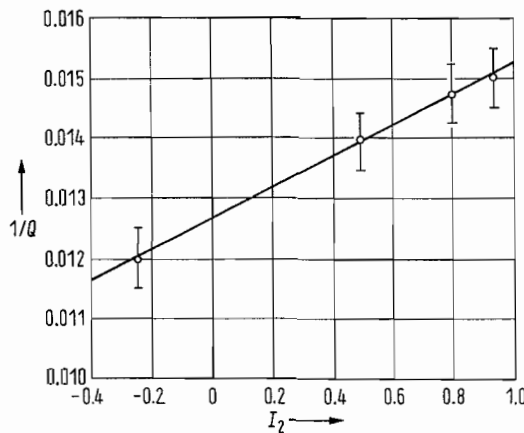


Fig. 4. Graph of measured values of Q^{-1} for modes of square plates and bars of ABS, against computed values of I_2 .

comparison with Fig. 2) we obtain

$$K_1'/K_1^0 \approx 1.26 \times 10^{-2}$$

and

$$\gamma \approx -0.21,$$

(3.1)

both being substantially constant over the frequency range 70 ... 140 Hz tested here. The corresponding point is plotted on Fig. 1; α is rather small, suggesting that ABS is "rubber-like". For other materials we have tested, either γ was smaller or the effect was more strongly masked by scatter, as explained in the previous paragraph. However we can say that no clear example of a material with positive γ has been encountered so far. A properly equipped experimenter will, we hope, take up the challenge and conduct a systematic survey of materials. This would no doubt reveal other isotropic materials with Q -variations comparable to, or possibly greater than, those of ABS. For the purpose of the present account, we need only note that the general validity of the approach is confirmed by Fig. 4 for small vibrations of at least one material; so we proceed to investigate theoretically the factors which can influence I_2 for a flat isotropic plate, regarding this simple system as a paradigm for more complicated ones which we could consider.

4. Influence of boundary conditions on I_2

We made the statement above that the simplest system to display the phenomenon of mode-to-mode variation of I_2 , and thus of Q , is an isotropic, rectangular thin plate with constant thickness and free edges. It is remarkable that, for polygonal isotropic plates, motion of the edges must be allowed in order to get the phenomenon. To examine the effect of boundary conditions in a general way, we first transform I_2 by integration by parts. We have

$$\frac{12 \rho \omega_0^2}{K_2^0} I_2 = - \int H \mathcal{G} w \, dA, \tag{4.1}$$

where $H(\mathbf{x}) = h^3(\mathbf{x})$, and w is normalised by

$$\int h w^2 \, dA = 1. \tag{4.2}$$

Noting eq. (2.10), we manipulate eq. (4.1), in a way analogous to that in Rayleigh [5], § 215, to give

$$\begin{aligned} - \frac{12 \rho \omega_0^2}{K_2^0} I_2 = & \tag{4.3} \\ = & \int \{ H_{xx} w_{yy} - 2 H_{xy} w_{xy} + H_{yy} w_{xx} \} w \, dA + \\ & + \oint H^2 \{ w_{yy} (w/H)_x - w_{xy} (w/H)_y \} n_{(x)} \, ds + \\ & + \oint H^2 \{ w_{xx} (w/H)_y - w_{xy} (w/H)_x \} n_{(y)} \, ds, \end{aligned}$$

where $(n_{(x)}, n_{(y)})$ are the components of the unit outward normal to the curve Γ bounding the plate. We may simplify the boundary integrals by writing them in terms of intrinsic edge coordinates, i.e. curvilinear coordinates n and s normal and tangential to the edge (see Rayleigh, loc. cit.), and the radius of curvature R of Γ :

$$\begin{aligned}
 & - \frac{12 \rho \omega_0^2}{K_2^0} I_2 = \\
 & = \int \{H_{xx} w_{yy} - 2H_{xy} w_{xy} + H_{yy} w_{xx}\} w \, dA + \\
 & + \oint H^2 \{(w/H)_n (w_{ss} + w_n/R) - \\
 & - (w/H)_s (w_{ns} - w_s/R)\} \, ds, \quad (4.4)
 \end{aligned}$$

where n is outward and R is taken positive for convex shapes. In the particular case of constant thickness, eq. (4.4) reduces to

$$\begin{aligned}
 - \frac{12 \rho \omega_0^2}{K_2^0} I_2 = H \oint \{w_n (w_{ss} + w_n/R) - \\
 - w_s (w_{ns} - w_s/R)\} \, ds, \quad (4.5)
 \end{aligned}$$

expressing the fact that the "total curvature" $\int \mathcal{G} w \, dA$ depends "only on the state of things at the edge" (Rayleigh, loc. cit.).

This form is convenient for discussing the effect upon I_2 of different boundary conditions. Consider first a plate restricted by $w=0$ on the boundary — this includes not only ideal "clamped" and "simply supported" boundary conditions but also practical "fixed" boundaries, which are usually somewhere between the two. Then $w_s=0$ on the boundary, and eq. (4.5) reduces to

$$- \frac{12 \rho \omega_0^2}{K_2^0} I_2 = H \oint (w_n^2/R) \, ds. \quad (4.6)$$

Thus if either the normal derivative $w_n=0$ on the boundary (clamped edges) or $1/R=0$ at all points of the boundary (polygonal shape), then $I_2=0$. This means that a flat isotropic plate of constant thickness exhibits no mode-dependence of internal damping if this has either

(a) a clamped boundary of any shape, or

(b) a polygonal boundary which is "fixed" ($w=0$) since, in either case, $I_2=0$ from eq. (4.6), and so from eq. (2.16)

$$Q^{-1} = K_1'/K_1^0,$$

a function of frequency alone.

If neither condition (a) nor (b) is satisfied but the boundaries are still fixed and are convex (e.g. a simply supported circular plate), then eq. (4.6) tells us that

$$\begin{aligned}
 I_2 < 0 \quad (\text{convex boundaries with } w=0). \\
 (4.7)
 \end{aligned}$$

(This gives an apparent paradox: we can regard a curved boundary, geometrically speaking, as the limit of a series of polygonal ones with an ever-increasing number of sides. But $I_2=0$ for all the polygonal plates, becoming non-zero in the limit. The mathematical loophole is that two non-interchangeable limits are tacitly being considered, the second one being that corresponding to the thin-plate approximation itself. Physically, the point can be resolved by examining the behaviour in the vicinity of a sharp corner whose angle straightens out to 180° . In a small neighbourhood of such a corner, the thin-plate approximation is violated, as it is near an edge. If we wanted to study the detailed behaviour very near the edge of a finite-thickness plate we would need to use a boundary-layer approach; see e.g. Love [8], § 297.)

For the case of free edges we can transform eq. (4.5) in various ways, with or without further integrations by parts, using the boundary conditions which are, in the same coordinates,

$$\begin{aligned}
 w_{nn} + \nu^0 (w_{ss} + w_n/R) & = 0 \\
 (\nabla^2 w)_n + (1 - \nu^0) (w_{ns} - w_s/R)_s & = 0, \quad (4.8)
 \end{aligned}$$

where ν^0 is Poisson's ratio as before. Such transformations are very useful in some particular situations, but apparently do not lead to useful general information in the absence of detailed solutions. But we may ask whether our results so far, including the numerical solutions of section 3 for a free square plate, suggest similarities between the damping behaviour of plates under different boundary conditions. At first sight we have, instead, a contrast: the majority of the computed free-plate modes have $I_2 > 0$ and comparable in magnitude to I_1 , whereas we have just shown that all plate modes under boundary conditions involving fixed edges ($w=0$), have $I_2 \leq 0$. The tendency for I_2 to be positive might be expected to hold for more general shapes, with free edges and $\nu^0 > 0$, if only because the effect of a non-zero Poisson's ratio is to tend, other things being equal, to produce "contrary curvatures", i.e. to make the Gaussian curvature negative.

The qualitative connection we are seeking appears to be provided, however, by the one free-plate mode which stands out as an exception to what has just been said, namely mode 3 (see Fig. 3). This has negative I_2 for all ν^0 . The reason is evidently the substantial central area over which $\mathcal{G}w$ is positive despite the absence of boundary constraints. The positive curvature is an inevitable consequence of having a single, closed, nodal curve. Such a "ring mode", where it occurred in a free plate of more

general shape, would likewise tend to have I_2 either negative or exceptionally small compared to other free modes. Thus its Q would be by far the best predictor of the Q 's of the modes which would occur if the edges were subsequently fixed in some way.

This may have a bearing, by qualitative analogy, on one of the problems related to the violin-maker's practice described in the Introduction. We asked there how one could hope to optimise in some way the performance of the finished instrument by minimising damping of certain free-plate modes: our results now hint at a possible explanation of why the free-plate mode Hutchins [1] considers most important is a "ring mode", that is, one with a single, closed, nodal curve like that of mode 3 of the square, isotropic plate. In an assembled violin, the plate boundaries are nearer fixed than free — see for example the time-average holograms of Jansson et al. [9] — and so perhaps the ring mode of the free plate acts as an especially suitable "barometer" for the behaviour of the plate after assembly. A different, additional sense in which this may be true will be suggested by the results of the next section.

5. Influence of thickness variations on I_2

We now turn to another question suggested directly by the violin-making observations, namely the effect of thickness variations in our flat isotropic plate on I_2 . While we can apply eq. (2.20) directly to numerical solutions of variable-thickness problems, such a "brute-force" approach requires a lot of computing effort for a small amount of information. Much more useful is a perturbation theory of the change in I_2 due to a small change in thickness distribution. Some care is needed in constructing such a theory in a self-consistent way, since we are already using an approximation of small damping so that the new approximation (small thickness change $\Delta h(\mathbf{x})$) leads to a double perturbation. In particular, eq. (2.14) is not a useful starting point.

Consider first the Rayleigh quotient (2.13) for the elastic problem in the form

$$\begin{aligned} \Omega(\nu^0) &\equiv K^0 \omega_0^2 = \\ &= \frac{\int h^3 (\nabla^2 w)^2 dA - 2(1 - \nu^0) \int h^3 \mathcal{G} w dA}{\int h w^2 dA} \end{aligned} \quad (5.1)$$

where

$$K^0 = 12 \rho / K_1^0 = 12 \{1 - (\nu^0)^2\} \rho / E^0. \quad (5.2)$$

Here K^0 appears only as a factor in the eigenvalue, so we absorb it conveniently into the quantity

$\Omega(\nu^0)$ and write $\Omega^0 = \Omega(\nu^0)$ for brevity. The only elastic constant affecting $w(\mathbf{x})$ is Poisson's ratio ν^0 .

We now introduce a small thickness perturbation in which $h(\mathbf{x})$ changes to $h(\mathbf{x}) + \Delta h(\mathbf{x})$. The stationary property of the quotient (5.1) immediately gives us an approximate expression for the resulting change $\Delta \Omega^0$, since the change induced in $w(\mathbf{x})$ does not contribute:

$$\begin{aligned} \Delta \Omega^0 &= K^0 \Delta(\omega_0^2) = \\ &= \frac{\int 3h^2 \Delta h \{(\nabla^2 w)^2 - 2(1 - \nu^0) \mathcal{G} w\} dA}{\int h w^2 dA} - \\ &\quad - \Omega^0 \frac{\int \Delta h w^2 dA}{\int h w^2 dA} + O\left(\frac{\Delta h}{h}\right)^2 \approx \\ &\approx \int \mathcal{F}(\mathbf{x}, \nu^0) \Delta h(\mathbf{x}) dA \end{aligned} \quad (5.3)$$

where $\mathcal{F}(\mathbf{x}, \nu^0)$, the perturbation-theory kernel for frequency squared, is given by

$$\mathcal{F}(\mathbf{x}, \nu^0) = 3h^2 \{(\nabla^2 w)^2 - 2(1 - \nu^0) \mathcal{G} w\} - \Omega^0 w^2 \quad (5.4a)$$

(evaluated with the unperturbed $w(\mathbf{x})$), and the elastic $w(\mathbf{x})$ is normalised by

$$\int h w^2 dA = 1 \quad (5.4b)$$

as in eq. (4.2).

We now go over to the viscoelastic problem to evaluate the change $\Delta(Q^{-1})$ due to changing $h(\mathbf{x})$ to $h(\mathbf{x}) + \Delta h(\mathbf{x})$. Note first that (with $\Omega = K \omega^2$)

$$\begin{aligned} \Delta \left[\frac{\text{Im}(\Omega)}{\Omega^0} \right] &= \Delta \left[\frac{\text{Im}(K)}{K^0} + \frac{\text{Im}(\omega^2)}{\omega_0^2} + O(\varepsilon^2) \right] = \\ &= \Delta(Q^{-1}) + O(\varepsilon^3) \end{aligned} \quad (5.5)$$

since

$$\Delta \left(\frac{\text{Im}(K)}{K^0} \right) = 0, \quad (5.6)$$

K being a material property. Here ε is a small parameter defined to bound the two small quantities of the problem:

$$Q^{-1} = O(\varepsilon) \quad \text{and} \quad |\Delta h/h| = O(\varepsilon). \quad (5.7)$$

Now eq. (5.3) is replaced in the viscoelastic problem by

$$\Delta \Omega(\nu) = \int \mathcal{F}(\mathbf{x}, \nu) \Delta h(\mathbf{x}) dA + O(\varepsilon^2),$$

and so

$$\begin{aligned} \text{Im}(\Delta \Omega) &= \nu' \int \frac{\partial \mathcal{F}(\mathbf{x}, \nu^0)}{\partial \nu^0} \times \\ &\quad \times \Delta h(\mathbf{x}) dA + O(\varepsilon^3), \end{aligned} \quad (5.8)$$

ν being the only material property influencing \mathcal{F} . Here $\nu' = \text{Im}(\nu)$, $\propto \gamma$ by eq. (2.27).

Thus, expanding the left hand side of eq. (5.5) we have

$$\begin{aligned} \Delta(Q^{-1}) &= \frac{\text{Im}[\Delta\Omega]}{\Omega^0} - \frac{\text{Im}(\Omega)\Delta(\Omega^0)}{(\Omega^0)^2} + O(\varepsilon^3) = \\ &= \frac{\nu'}{\Omega^0} \left\{ \int \Delta h \frac{\partial \mathcal{F}}{\partial \nu^0} dA - \right. \\ &\quad \left. - \frac{2(\int h^3 \mathcal{G} w dA)(\int \Delta h \mathcal{F} dA)}{\Omega^0} \right\} + O(\varepsilon^3), \end{aligned} \quad (5.9)$$

using eqs. (5.8), (5.3) and the viscoelastic analogue of eq. (5.1). Thus we may write

$$\Delta(Q^{-1}) = \frac{\nu'}{\Omega^0} \int \mathcal{D}(\mathbf{x}, \nu^0) \Delta h(\mathbf{x}) dA + O(\varepsilon^3) \quad (5.10)$$

where the kernel $\mathcal{D}(\mathbf{x}, \nu^0)$ for damping perturbations is given, noting eqs. (2.17 b) and (2.9), by

$$\mathcal{D}(\mathbf{x}, \nu^0) = \frac{\partial \mathcal{F}(\mathbf{x}, \nu^0)}{\partial \nu^0} + \frac{I_2}{1 - \nu^0} \mathcal{F}(\mathbf{x}, \nu^0). \quad (5.11)$$

The reason for casting the theory in this particular form is that it allows \mathcal{D} to be calculated

entirely from a knowledge of the elastic solution with unperturbed thickness. In Figs. 5 and 6 are presented some computed examples of the functions \mathcal{F} and \mathcal{D} , for the lowest four modes of a free square plate (Fig. 5), and simply supported square plate (Fig. 6), both having constant thickness and $\nu^0 = 0.25$. The numerical method is as described in Appendix 1, with $\partial \mathcal{F} / \partial \nu^0$ evaluated by numerical differentiation. In Figs. 5 and 6 the first column shows $w(\mathbf{x})$ for each mode, the second column the corresponding $\mathcal{F}(\mathbf{x})$ and the third column the corresponding $\mathcal{D}(\mathbf{x})$; the zero contour is marked in each case and the maximum and minimum values of each function are given below the picture.

We can make some simple deductions of a general nature from eqs. (5.10) and (5.11). First, we have $\Delta(Q^{-1}) = 0$ for $\Delta h \propto h$ from eq. (2.16) so that it is reassuring that

$$\int h \mathcal{D} dA = 0, \quad (5.12a)$$

as can be verified directly from eqs. (5.4) and (5.11), noting that \mathcal{F} depends on ν through w as well as explicitly. In the particular case of perturbation

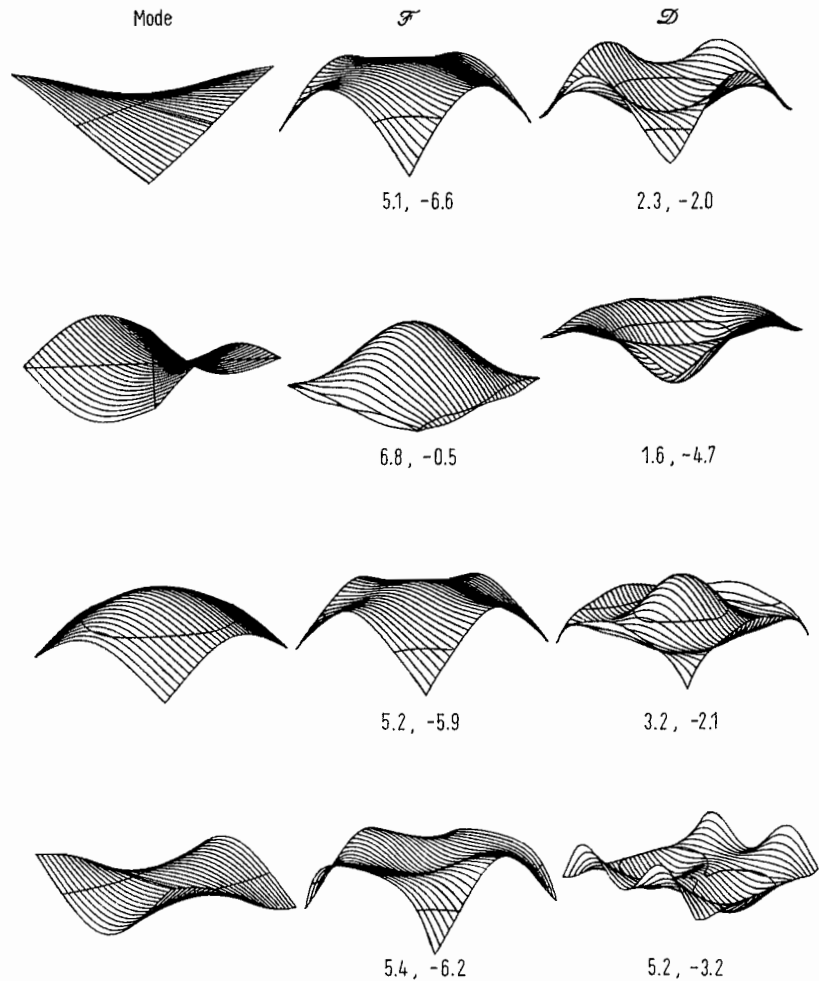


Fig. 5. Perturbation functions \mathcal{F} and \mathcal{D} for the gravest four modes of a free-edged, square, isotropic elastic plate, with $\nu^0 = 0.25$, with the maximum and minimum values of each function given beneath. An increase in thickness in a region of positive \mathcal{F} raises the frequency of the mode (and vice versa), while an increase in thickness in a region of positive \mathcal{D} increases Q for that mode in a material with negative γ , and vice versa. The numerical values are to be multiplied by $\Omega^0 h^{-1} L^{-2}$, where L^2 is plate area.

about a state of constant thickness, this means that

$$\int \mathcal{D} \, dA = 0 \quad (h(\mathbf{x}) = \text{constant}). \quad (5.12b)$$

Eq. (5.12a) holds for any boundary conditions, and is verified by the computed examples. (In fact, this is one useful check on the accuracy of the numerical method: see Appendix 1.)

Another point to be noticed in the pictures is that mode 3 for the free square plate again stands out as being different from the others: its \mathcal{D} has the opposite sign in the centre rather like that of the lowest mode of the supported square plate.

For constant-thickness plates with certain boundary conditions, the function \mathcal{D} reduces to a simple form. In particular, consider clamped plates of any shape, or fixed-edge polygonal plates, for which we have shown that

$$\int \mathcal{G} w \, dA = 0$$

(i.e. $I_2 = 0$; see section 4). For these cases it may readily be seen that $\partial w / \partial \nu^0 = 0$ and $d\Omega^0 / d\nu^0 = 0$

so that

$$\mathcal{D}(\mathbf{x}, \nu^0) = 6h^2 \mathcal{G} w(\mathbf{x}, \nu^0) \quad (5.13)$$

in this case. (Note the consistency with eq. (5.12b).) Here \mathcal{D} is sufficiently simple to be readily visualised from the mode shape as displayed by simple means such as Chladni patterns: it will be negative in the vicinity of two intersecting nodal lines (including sharp corners on the boundary) and positive in regions furthest removed from nodal lines. Thus if one were adjusting the thickness to try to reduce damping of a particular mode, while the plate was supported in such a way, one would immediately know where to remove material, provided that the sign of ν' (or γ) were known for the material of the plate.

We have cross-checked the correctness of the perturbation theory, and our computer programs for calculating plate eigenfunctions, by means of some comparisons between direct numerical solutions of variable-thickness problems and the predictions of perturbation theory. To maximise

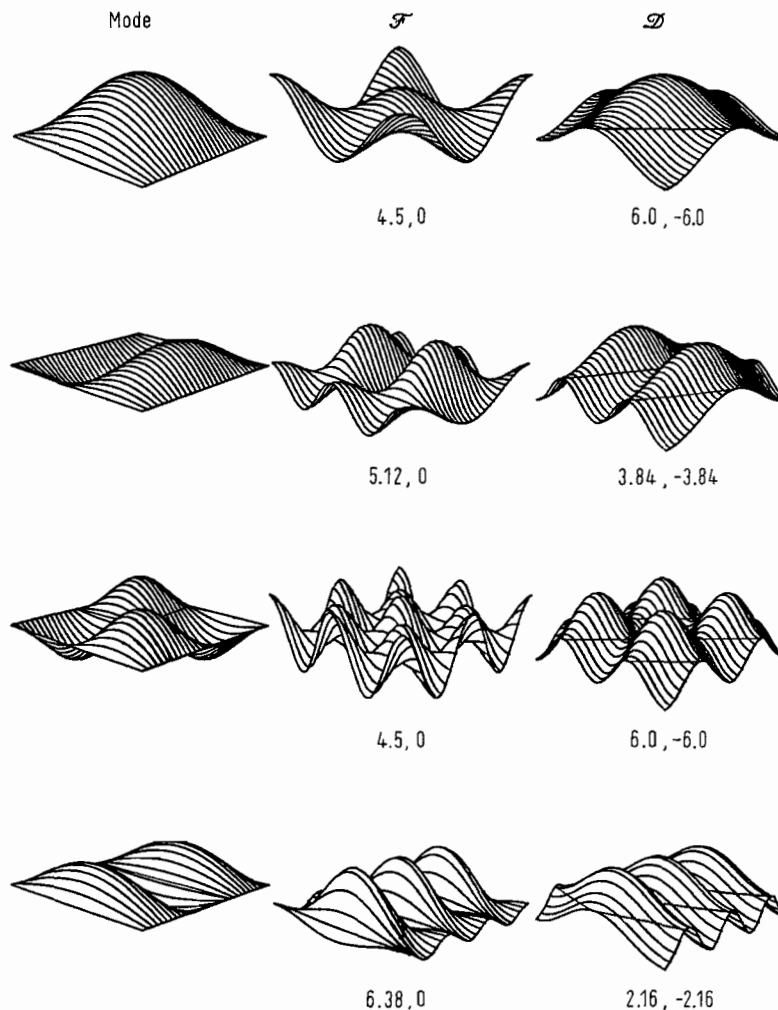


Fig. 6. Perturbation functions \mathcal{F} and \mathcal{D} for the gravest four modes of a square, simply-supported isotropic plate with $\nu^0 = 0.25$. Conventions are as in Fig. 5.

the effect we used a multiple of the function \mathcal{D} itself as the thickness perturbation Δh . We obtained agreement to within the accuracy of the calculations for small $\Delta h/h$ ratios. The results also give an indication of the range of validity of the perturbation theory, for functions Δh which vary on length scales comparable with those of \mathcal{D} : the predictions of $\Delta(Q^{-1})$ by the two methods typically differ by about 8% when the peak value of $|\Delta h/h|$ is 0.2.

Finally, we mention a general feature of the thickness perturbation theory which will carry over to more complicated systems including the curved orthotropic plates of the violin-maker, and which has direct relevance to violin-making practice. It is clear from the derivation of eq. (5.10) that the result of a similar procedure for any other system would take the same form, namely (for a given mode):

$$\Delta(Q^{-1}) \approx \int D(\mathbf{x}, K_1, \dots, K_N) \Delta h(\mathbf{x}) dA \quad (5.14)$$

with some function D involving the relevant viscoelastic constants K_n of the material in question. One thing we can reasonably state about this function D is that it will have very roughly the same

length-scale of variation in x, y as does the particular vibration mode in question. Thus eq. (5.14) tells us that a particular $\Delta h(\mathbf{x})$ will have a maximal effect, in one direction or the other, on Q for modes having about the same length-scale as $\Delta h(\mathbf{x})$.

Now in stringed musical instruments of less than top quality construction it is commonly found that the thickness distribution in the plates is irregular, with a typical length-scale of a few centimetres. Scraping these small "lumps" out can have a very substantial effect on the behaviour of the instrument. Our theory predicts that if we can measure some suitable frequency response curve of the plate before and after this scraping operation, we should see a particularly large change in a frequency range corresponding to modes with length-scales of a few centimetres. This effect has apparently been observed: Fig. 7 shows frequency response curves of a viola top plate, measured by the method described in Hutchins [10], before and after removal of lumps only a few tenths of millimetres in height. Note the marked changes in the range around 6 ··· 8 kHz.

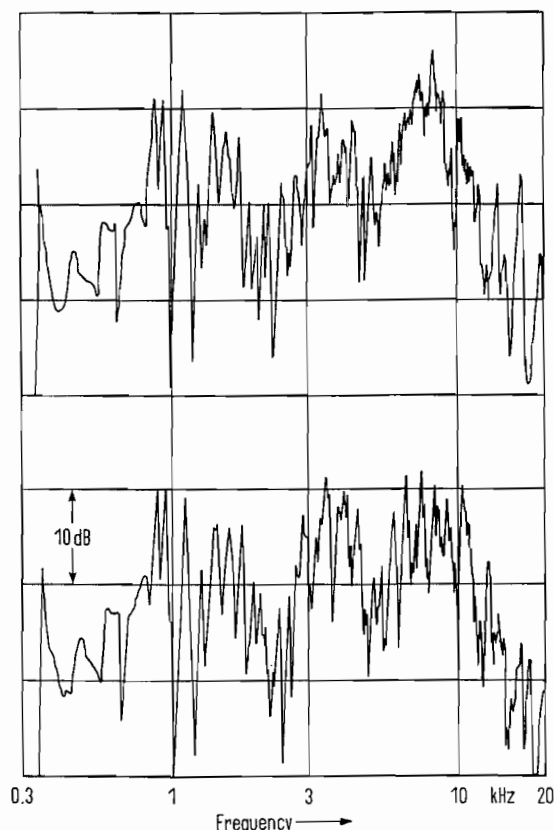


Fig. 7. Response curves of a viola top plate before and after small thickness irregularities were removed. The typical length-scale of these irregularities is a few cm, corresponding to modes with frequencies around 6 ··· 8 kHz. (Curves kindly supplied by C. M. Hutchins.)

6. Application of the theory to bars

We now leave isotropic plates and apply the theory to other systems, starting with the one which in view of its simplicity should logically have come first: the isotropic bar. According to classical beam theory, an isotropic bar with slowly-varying cross-section has a potential energy

$$V = \frac{1}{2} E^0 \int I w_{xx}^2 dx \quad (6.1)$$

and kinetic energy

$$\omega^2 T = \frac{1}{2} \rho \omega^2 \int A w^2 dx \quad (6.2)$$

where $A(x)$ is the cross-sectional area, $I(x)$ the moment of inertia of the cross-section about its centroid, E^0 is Young's modulus, ρ is density and the cross-sections are supposed all aligned with a principal axis of inertia in the plane of vibration. We can now apply our small-damping approximation to the Rayleigh quotient V/T as we did in deriving eq. (2.16), but in this case only one elastic constant enters V , so we get the altogether more trivial result

$$Q^{-1} = E'/E^0, \quad (6.3)$$

writing E' for the imaginary part of the complex Young's modulus as before. Thus Q is dependent on frequency alone, and is not influenced by mode shape, boundary conditions or slow variations in cross-section as was the case with plates.

One very important consequence of this is that observations of damping made on bars can measure only one viscoelastic constant, namely E'/E^0 (at least for frequencies sufficiently low for classical beam theory to be a reasonable approximation). So although only one measurement is needed to predict Q 's of all other bar modes, experiments with bars are not sufficient on their own to measure all relevant damping properties of an isotropic material which is to be vibrated in other ways (confirming the statement to this effect in section 3). An analogous result for orthotropic materials, such as wood, will be encountered in the next section.

We have verified this result experimentally: various modes of thin strips of ABS (which in plate form exhibited appreciable Q -variations; see section 3) were examined, and the Q 's were found to be all equal to within 5% whereas the Q 's of plate modes with different I_2 's differed by up to 20%.

To relate this discussion to the previous examination of plates it is instructive to calculate the value of I_2 for a long, thin plate (which will behave as a bar). Comparing eq. (6.3) to eq. (2.16), we require

$$\frac{E'}{E^0} = \frac{K_1'}{K_1^0} I_1 - \frac{K_2'}{K_2^0} I_2, \quad (6.4)$$

from which we can readily show with the aid of eqs. (2.9) and (2.18) that

$$I_2 = 2\nu^0/(1 + \nu^0). \quad (6.5)$$

To understand the physical origin of this value of I_2 , one must examine the deformation of the strip in more detail. It is clear that one principal axis of curvature will run along the strip. Suppose the principal radii of curvature along and across the strip are R_1 , and R_2 respectively. Then

$$1/R_2 = -\nu^0/R_1, \quad (6.6)$$

since the thin strip curls across its width by approximately the right amount for static equilibrium under the applied longitudinal curvature. (R_2 minimizes the integrand of eq. (2.8), for given R_1 .) We can recover eq. (6.5) by substituting eq. (6.6) into the expression (2.17b) for I_2 , noting eqs. (2.11) and (2.13).

There is one possible way of measuring γ or ν' for an isotropic material by observations of strips, and that is by measuring Q 's of high modes, of sufficiently short length-scale that the effects of shear motion and rotatory inertia become appreciable. Timoshenko beam theory must then be used in place of classical beam theory. In that case, the potential energy is, from Washizu [11], section 7.7

and appendix C

$$V = \frac{1}{2} \int \{E^0 I(x) u_x^2 + \mu^0 \kappa^2 A(x) [w_x + u]^2\} dx, \quad (6.7)$$

and the kinetic energy is

$$\omega^2 T = \frac{1}{2} \rho \omega^2 \int \{A w^2 + h^3 I(x) u^2\} dx, \quad (6.8)$$

where the displacement components of a particle in the beam are $(zu(x), 0, w(x))$, E^0 is Young's modulus, μ^0 is the shear modulus, κ^2 is the Timoshenko shear coefficient (a dimensionless constant) and $A(x)$ and $I(x)$ are cross-sectional area and moment of inertia as in eqs. (6.1) and (6.2). Since two independent constants now enter, we can derive a result like (2.16) or (2.20), in the same way as before. There is a problem, however: some writers, e.g. Mindlin [12], have suggested that the Timoshenko shear coefficient κ^2 should depend on Poisson's ratio. If this were the case, the form of the dependence would need to be known if one were to attempt to measure γ in this way. We shall not pursue the matter further here; we hope to put it to experimental test soon. To close this section, we point out in passing that a similar technique can be employed if high modes of plates are to be investigated; we can then use an extended plate theory such as Mindlin's [12], which takes account of shear and rotatory inertia (see Appendix 2). This theory also suffers from the problem of the possible dependence of a "shear coefficient" on Poisson's ratio.

7. Application of the theory to orthotropic plates and strips

The next system worthy of consideration, particularly in view of the violin-making observations motivating this study, is the flat orthotropic plate. We again use classical thin-plate theory: with a suitable choice of coordinate axes the potential energy is

$$V = \frac{1}{2} \int h^3 \{D_1^0 w_{xx}^2 + D_2^0 w_{xx} w_{yy} + D_3^0 w_{yy}^2 + D_4^0 w_{xy}^2\} dA \quad (7.1)$$

and the kinetic energy is

$$\omega^2 T = \frac{1}{2} \rho \omega^2 \int h w^2 dA, \quad (7.2)$$

where D_1^0 , D_2^0 , D_3^0 and D_4^0 are four independent elastic moduli whose precise relation to other moduli we need not go into here; see Hearmon [13]. (We assume that our plate is cut from an orthotropic material in such a way as to include two of the symmetry axes of the material, or rather that

the plate as a whole has the corresponding symmetry properties, as with the carbon-fibre sandwich described by Haines and Chang [14].) For viscoelastic problems, our small-damping approximation then leads to the analogue of eq. (2.16):

$$Q^{-1} \approx \left(\frac{D_1'}{D_1^0}\right) J_1 + \left(\frac{D_2'}{D_2^0}\right) J_2 + \left(\frac{D_3'}{D_3^0}\right) J_3 + \left(\frac{D_4'}{D_4^0}\right) J_4, \quad (7.3)$$

where

$$\begin{aligned} J_1 &= \frac{D_1^0 \int h^3 w_{xx}^2 dA}{\rho \omega_0^2 \int h w^2 dA}, \\ J_2 &= \frac{D_2^0 \int h^3 w_{xx} w_{yy} dA}{\rho \omega_0^2 \int h w^2 dA}, \\ J_3 &= \frac{D_3^0 \int h^3 w_{yy}^2 dA}{\rho \omega_0^2 \int h w^2 dA}, \\ J_4 &= \frac{D_4^0 \int h^3 w_{xy}^2 dA}{\rho \omega_0^2 \int h w^2 dA}, \end{aligned} \quad (7.4)$$

where $\omega_0^2 = V/T$ as usual, so that, in place of eq. (2.18),

$$J_1 + J_2 + J_3 + J_4 = 1. \quad (7.5)$$

Eq. (7.3) may be used in a similar way to eq. (2.16): we could examine the effect on Q of different mode shapes, boundary conditions and (by developing the result equivalent to eq. (5.10)) thickness distributions.

To use this information for a given material, we need measurements of the four complex material parameters D_n . We first enquire how to make such measurements. As we noted in the context of isotropic plates, thin strips are easier to work with than plates, so it is natural to ask how many of the constants may be determined from observations of strips. By an analysis similar to that of section 6, we find that for strips cut from a thin plate along the principal axes of the material we can measure the real and imaginary parts of

$$\begin{aligned} E_x &\equiv D_1 - D_2^2/4D_3 \quad \text{and} \\ E_y &\equiv D_3 - D_2^2/4D_1 \end{aligned} \quad (7.6)$$

for strips cut along the x and y axes respectively. For a thin strip cut at an angle θ to one principal axis (the y -axis), the constant whose real and imaginary parts we can measure is

$$E_\theta \equiv D_4(4D_1D_3 - D_2^2)/4\Delta(\theta), \quad (7.7)$$

where

$$\begin{aligned} \Delta(\theta) &\equiv D_4(D_1 \cos^4 \theta + D_3 \sin^4 \theta) + \\ &+ (4D_1D_3 - D_2^2 - D_2D_4) \sin^2 \theta \cos^2 \theta. \end{aligned}$$

(E_θ is most easily calculated as the expression within braces in eq. (7.1), minimized with respect

to the local values of w_{xx} , w_{xy} and w_{yy} for a given longitudinal curvature

$$\begin{aligned} 1/R_{\text{long}} &\equiv w_{xx} \sin^2 \theta + 2w_{xy} \cos \theta \sin \theta + \\ &+ w_{yy} \cos^2 \theta, \end{aligned}$$

and multiplied by R_{long}^2 .)

We note immediately that $\Delta(\theta)$ is a linear combination of $\sin^4 \theta$, $\cos^4 \theta$ and $\sin^2 \theta \cos^2 \theta$ only; it follows that only three independent combinations of D_1, \dots, D_4 can be measured from strips cut from a thin plate — for instance E_x, E_y and $E_{\pi/4}$. Thus strips exhibit a degeneracy similar to that already noted in Section 6 for isotropic strips. Presumably one would find similar limitations for bars of arbitrary cross-section.

Measurements on wood made to date (for example Barducci and Pasqualini [2]) have used thin strips cut along and across the grain, so that they have determined E_x and E_y of eq. (7.6). We have just seen that at least two more constants must be measured before a full discussion of the damping properties of wood may be attempted, and that only one more can be obtained from strip measurements. We are currently exploring the possibilities offered by plate measurements analogous to those of Section 3; and preliminary experimental results appear consistent with eq. (7.3).

Some writers (e.g. Schelleng [15]) have used approximate interrelations between the real constants D_n^0 , and have assumed these to carry over to the imaginary parts D_n' . These assumptions should be tested: it would be very convenient if they turned out to be valid, since they would then reduce the number of degrees of freedom of the problem and thus make it more amenable to the sort of arguments we have used about isotropic plates. One immediate use for the measurements would be to aid the promising efforts being made by Haines [14] and others to duplicate the properties of the spruce wood used in musical instruments with synthetic materials.

8. Conclusions and directions of further work

We have presented a general formalism for discussing the internal damping of vibration modes of structures, provided that linear theory is appropriate and that this damping is small. We have applied this method to some simple systems, and have seen that behaviour similar to that observed in violin plates may be expected even in flat, isotropic plates. Thus such behaviour (dependence of Q upon mode shape, geometry and

boundary conditions) could be significant in engineering situations where the precise level of internal damping is important: for a given isotropic material we have shown that measurement of a single parameter (the imaginary part of Poisson's ratio, or equivalently one of the parameters α , γ in eqs. (2.21, 2)) is needed to find out if this is the case. A method of measuring this parameter has been described and illustrated by experiments on ABS plastic sheet.

Since flat, isotropic plates are easier to discuss than are wooden violin plates, we have suggested some possible analogies between the behaviour of the two which may cast some light on the observed violin-plate behaviour (sections 4, 5). We emphasise that we have not yet done any detailed work on curved orthotropic shells, and an important direction of further work is to do so, to find out whether these analogies hold up. Other limitations of the present discussion should also be kept in mind: the use of classical plate theory restricts the detailed conclusions so far reached to the lower normal modes of the plates in question, and the discussion of the effects of variable thickness is restricted to slowly-varying thickness. We hope to examine in due course the behaviour of plates when these last two restrictions do not apply, since there is a suggestion of interesting behaviour from observations of violin plates (see end of section 5).

We finally mention a feature of violin construction which we have not yet touched on, which also influences the damping behaviour of the plates and is of some significance to engineering applications. This is the bass-bar, a wooden strut glued to the underside of the front plate of a violin. The profile of this bar influences strongly the shape, frequency and damping of the vibration modes of the plate [1]. Since strutted plates are common in engineering situations (and in other musical instruments), a discussion of the effect of this could be of relevance in a wide area of acoustics. We hope to supply such a discussion soon.

Acknowledgements

We would like to thank the Science Research Council and Clare College for financial support, and the Cambridge University Engineering Department for making experimental facilities available to us. In particular, we thank J. E. Ffowes Williams, J. Billingsley, D. R. S. Hedgeland and J. L. Moughton for valuable and unstinted assistance with the experimental work described here. Imperial Chemical Industries Ltd. kindly supplied samples of some

plastics. We are also indebted to many colleagues for helpful discussion and comments — in particular D. W. Haines, R. Hill, C. M. Hutchins, J. W. Hutchinson, M. J. Lighthill and G. P. Parry.

Appendix 1

Computations of eigenmodes of a rectangular isotropic elastic plate

To obtain the information in Figs. 2, 3, 5 and 6 we have computed eigenmodes of rectangular isotropic elastic plates by a finite-difference method. The equation of motion of the plate, from eq. (5.1),

$$\begin{aligned} \nabla^2(H \nabla^2 w) - (1 - \nu^0) \times \\ \times (H_{xx} w_{yy} - 2H_{xy} w_{xy} + H_{yy} w_{xx}) = \\ = h \Omega^0 w, \end{aligned} \quad (\text{A } 1.1)$$

where $H(\mathbf{x}) = h^3(\mathbf{x})$, was approximated by the simplest centred-difference form in terms of w -values stored on a uniform rectangular grid. The boundary conditions (e.g. eqs. (4.8) for free boundaries) were similarly represented. This discrete problem was then solved by a matrix manipulation method. It was transformed into a matrix eigenvalue-eigenvector problem, which was solved by a standard inverse-power-iteration procedure once the relevant matrix had been calculated. With the matrix subroutine used so far, computer storage limitations necessitate a fairly coarse grid for this approach — we used a 16×16 grid. (More powerful matrix routines are currently becoming available, however.)

The results have been checked, in various respects, by the following four methods.

(a) The discrete problem was solved by a different method, an iterative over-relaxation procedure, to check the coding of the program. The two methods agree to the accuracy of the calculations, so we are assured that the discrete problem is being correctly solved.

(b) Results were compared with known analytic solutions: Rayleigh [5], § 226, has shown that for $\nu^0 = 0$, certain modes of a free-edged rectangular plate can be found exactly. Our program produces agreement with these to an accuracy of three figures in $w(\mathbf{x})$. This checks the truncation error of the finite-difference method.

(c) The results were checked against eqs. (5.12), for perturbation functions \mathcal{D} calculated by finite-difference methods from the computed $w(\mathbf{x})$. This confirmed the calculation to the same accuracy as check (b).

(d) Most powerfully of all, we have checked the predictions of the thickness-perturbation theory of section 5, using perturbation functions as calculated in (c) above, against direct numerical solution of variable-thickness problems. This last, producing agreement to the expected accuracy, confirms the perturbation theory itself as well as the numerical technique.

The numerical procedure described above can also be used for flat, orthotropic plates. We have obtained the predictions of J_1 , J_2 , J_3 and J_4 (section 7) necessary for an experimental determination of the constants D_n'/D_n^0 from eq. (7.3). We hope to report the details in due course, when more experiments have been done on orthotropic plates.

Appendix 2

A reference list of potential and kinetic energy integrals for some of the systems to which our methods could be applied. The kinetic energy is denoted by $\omega_0^2 T$.

1. Classical beam theory

$$V = \frac{1}{2} E^0 \int I w_{xx}^2 dx,$$

$$T = \frac{1}{2} \rho \int A w^2 dx,$$

where $A(x)$ is cross-sectional area, $I(x)$ is the moment of inertia of the cross-section about its centroid, E^0 is Young's modulus and ρ is density.

2. Timoshenko beam theory [11]

$$V = \frac{1}{2} \int \{E^0 I u_x^2 + \mu^0 \kappa^2 A [w_x + u]^2\} dx,$$

$$T = \frac{1}{2} \rho \int \{I u^2 + A w^2\} dx,$$

where μ^0 is the shear modulus, κ^2 is the Timoshenko shear coefficient, and the displacement components of a particle in the beam are approximately $\{z u(x), 0, w(x)\}$.

3. Classical isotropic plate theory

$$V = \frac{1}{24} \int h^3 \{K_1^0 (\nabla^2 w)^2 - K_2^0 (w_{xx} w_{yy} - w_{xy}^2)\} dA,$$

$$T = \frac{1}{2} \rho \int h w^2 dA,$$

where $h(\mathbf{x})$ is thickness, ρ is density,

$$K_1^0 = E^0 / (1 - \nu^0),$$

and

$$K_2^0 = 2E^0 / (1 + \nu^0) = 4\mu^0,$$

where ν^0 is Poisson's ratio.

4. Extended plate theory (e.g. Mindlin [12]):

$$V = \frac{1}{24} \int [h^3 \{K_1^0 (u_x + v_y)^2 - K_2^0 [u_x v_y - u_y v_x - \frac{1}{4} (u_y - v_x)^2]\} + 12\mu^0 \kappa^2 h \{(w_x + u)^2 + (w_y + v)^2\}] dA,$$

$$T = \rho \int \left\{ \frac{h^3}{24} (u^2 + v^2) + \frac{h}{2} w^2 \right\} dA,$$

where κ^2 is Mindlin's shear coefficient, and the displacement components of a particle in the plate are approximately $\{z u(x, y), z v(x, y), w(x, y)\}$.

5. Classical orthotropic plate theory

$$V = \frac{1}{2} \int h^3 \{D_1^0 w_{xx}^2 + D_2^0 w_{xx} w_{yy} + D_3^0 w_{yy}^2 + D_4^0 w_{xy}^2\} dA,$$

$$T = \frac{1}{2} \rho \int h w^2 dA,$$

where D_1^0 , D_2^0 , D_3^0 , and D_4^0 are four independent elastic moduli (whose precise meaning in the case where the plate is made of homogeneous material may be found in Hearmon [13]).

6. Classical theory of general isotropic shells [16], [17]:

$$V = \frac{1}{24} \int \{h^3 E^{\alpha\beta\gamma\delta} R_{\alpha\beta} R_{\gamma\delta} + 12h E^{\alpha\beta\gamma\delta} \Gamma_{\alpha\beta} \Gamma_{\gamma\delta}\} dA,$$

$$T = \frac{1}{2} \rho \int h (w^2 + g^{\alpha\beta} u_\alpha u_\beta) dA,$$

where

$$E^{\alpha\beta\gamma\delta} = (K_1^0 - \frac{1}{2} K_2^0) g^{\alpha\beta} g^{\gamma\delta} + \frac{1}{2} K_2^0 g^{\alpha\gamma} g^{\beta\delta}$$

is the contravariant tensor of elastic moduli, $g^{\alpha\beta}$ is the contravariant metric tensor of the undeformed shell, $\Gamma_{\alpha\beta}$ is the covariant in-surface strain tensor, and $R_{\alpha\beta}$ is the covariant tensor of curvature changes. The Greek indices run from 1 to 2 and correspond to general curvilinear coordinates in the middle surface of the shell.

This much applies to completely general, thin shells. If we wish to apply it in practice, however, we need strain-displacement relations, and it is expedient here to use the shallow-shell approximation. Then if the displacement components on the middle surface are (u_1, u_2, w) we have

$$\Gamma_{\alpha\beta} = \frac{1}{2} (u_{\alpha,\beta} + u_{\beta,\alpha}) + b_{\alpha\beta} w,$$

$$R_{\alpha\beta} = -w_{,\alpha\beta}$$

where $b_{\alpha\beta}$ is the curvature tensor; note that $w_{,\alpha\beta} \approx w_{,\beta\alpha}$ for shallow shells [17].

(Received October 16th, 1976.)

References

- [1] Hutchins, C. M., Thate lusive 'clear full ring'. *Catgut Acoust. Soc. Newsletter* **5** [1966], 4. See also *ibid.* **16** [1971], 15*, and **19** [1973], 17.
- [2] Barducci, I. and Pasqualini, G., Misura dell'attrito interno e delle costanti elastiche del legno. *Il Nuovo Cim.* **5** [1948], 416*.
- [3] Bland, D. R., *Theory of linear viscoelasticity*. Pergamon, London 1960.
- [4] Scanlan, R. H., Linear damping models and causality in vibrations. *J. Sound Vib.* **13** [1970], 499.
- [5] Rayleigh, J. W. S., *The theory of sound*, second edition. Macmillan, London 1894, and Dover, New York 1945.
- [6] Snowdon, J. C., *Vibration and shock in damped mechanical systems*. Wiley, New York-London 1968.
- [7] Lazan, B. J., *Damping of materials and members in structural mechanics*. Pergamon, London 1968.
- [8] Love, A. E. H., *A treatise on the mathematical theory of elasticity*. Cambridge University Press, Cambridge 1927.
- [9] Jansson, E., Molin, N. E. and Sundin, H., Resonances of a violin body studied by hologram interferometry and acoustical methods. *Physica Scripta* **2** [1970], 243*. See also Reinicke, W. and Cremer, L., Application of holographic interferometry to vibrations of the bodies of string instruments. *J. Acoust. Soc. Amer.* **48** [1970], 988*.
- [10] Hutchins, C. M., Stetson, K. A. and Taylor, P. A., Clarification of "free plate tap tones" by hologram interferometry. *Catgut Acoust. Soc. Newsletter* **16** [1971], 15*.
- [11] Washizu, K., *Variational methods in elasticity and plasticity*. Pergamon, London 1968.
- [12] Mindlin, R. D., Influence of rotatory inertia and shear on flexural motions of isotropic elastic plates. *J. Appl. Mech.* **18** [1951], 31.
- [13] Hearmon, R. F. S., *Introduction to applied anisotropic elasticity*. Oxford University Press, London 1961.
- [14] Haines, D. W. and Chang, N., Application of graphite composites in musical instruments. *Catgut Acoust. Soc. Newsletter* **23** [1975], 13.
- [15] Schelleng, J. C., Acoustical effects of violin varnish. *J. Acoust. Soc. Amer.* **44** [1968], 1175*.
- [16] Koiter, W. T., A consistent first approximation in the general theory of thin elastic shells. *International Union of Theoretical and Applied Mechanics, Delft Symposium, 1959* (edited by W. T. Koiter).
- [17] Green, A. E. and Zerna, W., *Theoretical elasticity*. Oxford University Press, London 1954.

* Republished in *Benchmark Papers in Acoustics* (series editor, R. Bruce Lindsay), vols. **5** and **6**: *Musical Acoustics, violin family*, edited by C. M. Hutchins. Wiley-Halsted, New York-London, 1975 and 1976.